CWI Quarterly Volume 10 (3&4) 1997, pp. 337 – 352

Error Estimates and Numerical Experiments for Streamline-Diffusion-Type Methods on Arbitrary and Shishkin Meshes

Martin Stynes
Department of Mathematics, University College Cork, Western Road, Cork, Ireland

Lutz Tobiska
Institut für Analysis und Numerik, Otto-von-Guericke-Universität, Magdeburg, Postfach 4120 D-39016 Magdeburg, Germany

We analyse and numerically study streamline-diffusion finite element methods applied to a singularly perturbed convection-diffusion two-point boundary value problem whose solution has a single boundary layer. We first consider arbitrary meshes, then in analysing the scheme on a Shishkin mesh, we consider two formulations on the fine part of the mesh: the usual streamline diffusion upwinding and the standard Galerkin method. The error estimates we report are given in the discrete L^∞ norm and in particular describe the dependence of the error on the user-chosen parameter τ_0 specifying the mesh. When τ_0 is too small, the error becomes $O(1)$, but for τ_0 above a certain threshold value, the error is small and increases very slowly as a function of τ_0. Numerical tests support the theoretical results for the L^∞ norm.

1. Introduction

We consider the singularly perturbed boundary value problem

$$(Lu)(x) := -\varepsilon u''(x) + a(x)u'(x) = f(x) \quad \text{for } x \in (0,1), \tag{1.1}$$
$$u(0) = u(1) = 0,$$

where ε is a small positive parameter, $a(x) > \alpha > 0$ for all $x \in [0,1]$ and some constant α, and the functions a and f are sufficiently smooth. The solution of (1.1) has a boundary layer at $x = 1$ (see, e.g., [12, 13]).

Convection-diffusion problems of this type arise in linearised versions of the Navier-Stokes equations, so it is important to devise effective methods for their numerical solution. Many such methods have been proposed in the literature; see [13] for a survey.

In this context, one of the most commonly used numerical methods is the streamline-diffusion finite element method (SDFEM), which combines good stability properties with high accuracy. It was introduced by Hughes and Brooks [4] and its convergence properties have been studied by many authors [5, 7, 10, 11, 19]. The method has also been extended to much more complicated problems, such as the incompressible Navier-Stokes equations [6, 8, 18]. Nevertheless, the precise behaviour of the SDFEM on nonuniform meshes is unknown. As a first step towards a better understanding of the properties of the SDFEM on meshes that are designed for convection-diffusion problems, we shall give a sharp analysis of its behaviour when it is used to solve (1.1) on arbitrary and special meshes.

Recently, several upwind finite difference methods for (1.1) have been studied on special meshes [1, 9, 16] and ε-uniform convergence results have been proved. The difference schemes produced by the SDFEM differ from these upwind methods. The most prominent difference is that, unlike the methods in [1, 9, 16], the SDFEM scheme loses consistency at any mesh point where the local mesh is nonuniform.

In this paper, we shall develop techniques sharper than those of [1, 9, 16] to analyse the SDFEM. In particular, we are able to make precise the relationship between the error in the numerical solution and the user-chosen mesh parameter for the well-known Shishkin mesh. Previous work on the effect of varying this parameter has been confined to numerical experiments (see, e.g., [2], where an alternative difference method is used on the Shishkin mesh).

Let our mesh be defined by $0 = x_0 < x_1 < \ldots < x_N = 1$, where N is some positive integer. For $i = 1, \ldots, N$ we set $x_{i-1/2} = (x_{i-1} + x_i)/2$ and $h_i = x_i - x_{i-1}$. Let $H = \max_i h_i$. Given a mesh function $v = \{v_i\}$, define the forward and backward difference operators D_+ and D_- by

$$D_+ v_i := \frac{v_{i+1} - v_i}{h_{i+1}} \quad \text{and} \quad D_- v_i := \frac{v_i - v_{i-1}}{h_i},$$

respectively.

Let ϕ_i, for $i = 0, \ldots, N$, be the usual basis functions for the space of piecewise linear functions, viz.,

$$\phi_i(x) := \begin{cases} \dfrac{x - x_{i-1}}{h_i} & \text{for} \quad x \in [x_{i-1}, x_i] \\ \dfrac{x_{i+1} - x}{h_{i+1}} & \text{for} \quad x \in [x_i, x_{i+1}] \\ 0 & \text{for} \quad x \notin [x_{i-1}, x_{i+1}] \end{cases} .$$

Set $V^N := \text{span}\{\phi_1, \ldots, \phi_{N-1}\}$. The SDFEM for solving (1.1) is defined as follows:

Find $u_N \in V^N$ such that, for all $v_N \in V^N$,

$$\sum_{i=1}^{N} \int_{x_{i-1}}^{x_i} (\varepsilon u_N' v_N' + a u_N' v_N + a u_N' \delta_{i-1/2} a v_N')\, dx$$
$$= \sum_{i=1}^{N} \int_{x_{i-1}}^{x_i} f(v_N + \delta_{i-1/2} a v_N')\, dx. \tag{1.2}$$

Here $\delta_{i-1/2}$ is called the streamline diffusion parameter, or SD-parameter for short. If $\delta_{i-1/2} = 0$ for $i = 1, \ldots, N$, then we get the standard Galerkin discretization for (1.1), which is known to produce nonphysical oscillations unless the mesh is very fine.

In order to evaluate the integrals in (1.2) we apply the standard midpoint rule

$$\int_{x_{j-1}}^{x_j} \Psi(x)\, dx \sim (x_j - x_{j-1}) \Psi(x_{j-1/2}).$$

Let the discrete solution of (1.2) be

$$u_N(x) = \sum_{i=0}^{N} u_i \phi_i(x).$$

Then, taking $v_N = \phi_i$ for $i = 1, \ldots, N-1$ in (1.2), we get the scheme

$$L^N(u_i) = \lambda_{i+1/2} f_{i+1/2} + \mu_{i-1/2} f_{i-1/2}\ , \quad \text{for } i = 1, \ldots, N-1, \tag{1.3}$$
$$u_0 = u_N = 0\ ,$$

where

$$\begin{aligned} L^N(u_i) \quad &:= \quad -\frac{\varepsilon}{h_i}\{D_+ u_i - D_- u_i\} \\ &\quad +\lambda_{i+1/2} a_{i+1/2} D_+ u_i + \mu_{i-1/2} a_{i-1/2} D_- u_i\ , \end{aligned} \tag{1.4}$$

and

$$\lambda_{i+1/2} := \frac{h_{i+1} - 2\delta_{i+1/2} a_{i+1/2}}{2h_i}\ , \quad \mu_{i-1/2} := \frac{h_i + 2\delta_{i-1/2} a_{i-1/2}}{2h_i}\ .$$

When ε is small relative to the local meshsize, a standard way of stabilizing this scheme is to choose $\delta_{i+1/2}$ according to the formula

$$\delta_{i+1/2} = h_{i+1}/(2a_{i+1/2}). \tag{1.5}$$

For this special choice the scheme (1.3) becomes

$$\begin{aligned} L_1^N(u_i) \quad &:= \quad -\frac{\varepsilon}{h_i}\{D_+ u_i - D_- u_i\} + a_{i-1/2} D_- u_i \\ &= \quad f_{i-1/2}\ , \quad \text{for } i = 1, \ldots, N-1, \\ u_0 \quad &= \quad u_N = 0\ . \end{aligned} \tag{1.6}$$

If the local meshsize is small enough — in particular if $a_{i+1/2}h_{i+1} < 2\varepsilon$ — then the standard Galerkin method works well, so it is possible to choose $\delta_{i+1/2} = 0$. Thus the second special scheme that we consider is (1.3) with the choice

$$\delta_{i+1/2} = \begin{cases} 0, & \text{if} \quad a_{i+1/2}h_{i+1} < 2\varepsilon, \\ \dfrac{h_{i+1}}{2a_{i+1/2}}, & \text{if} \quad a_{i+1/2}h_{i+1} \geq 2\varepsilon. \end{cases} \tag{1.7}$$

This generates a scheme whose difference operator we call L_2^N.

In all variations of the SDFEM, one always chooses $\delta_{i+1/2}$ in such a way that $0 < \delta_{i+1/2} \leq h_{i+1}/(2a_{i+1/2})$. Thus we shall assume that $\lambda_{i+1/2} \geq 0$ and $\mu_{i+1/2} \geq 1/2$. Moreover, we add a condition that guarantees that the difference scheme satisfies a discrete maximum principle (Lemma 2.2 below): we shall henceforward assume that the parameters λ and μ satisfy

$$\frac{\varepsilon}{h_i a_{i+1/2}} \geq \lambda_{i+1/2} \geq 0 \quad \text{and} \quad \mu_{i+1/2} \geq 1/2 \quad \text{for all } i. \tag{1.8}$$

Both our special choices (L_1^N and L_2^N) satisfy (1.8).

REMARK 1.1. *When the functions a and f are constants, then the choice*

$$\delta_{i+1/2} = \frac{h_{i+1}}{2a}\left(\coth\frac{ah_{i+1}}{2\varepsilon} - \frac{2\varepsilon}{ah_{i+1}}\right) \tag{1.9}$$

yields the exact solution at all nodes [3]. For this choice of δ, if the mesh is fixed then

$$\lim_{\varepsilon\to 0^+} \delta_{i+1/2} = \frac{h_{i+1}}{2a}.$$

That is, the choice (1.5) is essentially the limiting case of (1.9) when ε is small compared with the local meshsize.

The plan of the paper is the following. First, in Section 2, we outline an analysis of the scheme on a general mesh. In Section 3 we study its behaviour on a Shishkin mesh, which is a piecewise uniform mesh. The transition point that separates the coarse and fine portions of the Shishkin mesh is given by

$$1 - \tau := 1 - \min\left\{\frac{1}{2}, \frac{\tau_0}{\alpha}\varepsilon \log N\right\},$$

where τ_0 is a user-chosen parameter. While Shishkin meshes have been used to compute numerical solutions of many singularly perturbed differential equations, no previous analysis has revealed the relationship between τ_0 and the error in the computed solution. We state the results of such an analysis here. In Section 4 we describe numerical experiments that demonstrate both the accuracy obtained when using the Shishkin mesh and the sharpness of the theoretical relationship between the error and τ_0 that was proved in Section 3.

Full details of the analysis outlined here can be found in [17].

Notation. Throughout the paper C will denote a generic positive constant that is independent of ε and the mesh. In the particular case of a Shishkin mesh (Sections 3 and 4) it will also be independent of τ_0. When we write, e.g., $g_j = O(\varepsilon h_j)$, we mean that $|g_j| \leq C\varepsilon h_j$ (and note that C is independent of j).

2. Error Estimate on an Arbitrary Mesh

The following ingredients are essential in the analysis leading to our error estimates.

– Decomposition of the exact solution (1.1) into smooth and layer parts, which can be found in [9]:

LEMMA 2.1. *The solution u of (1.1) can be decomposed as $u(x) = G(x) + E(x)$ on $[0,1]$, where for any prescribed finite order q and $0 < x < 1$, the smooth part G satisfies $LG(x) = f(x)$ and*

$$|G^{(k)}(x)| \leq C \quad \text{for } k = 0, 1, \ldots, q\,, \tag{2.1}$$

while the layer part E satisfies $(LE)(x) = 0$, and

$$|E^{(k)}(x)| \leq C\,\varepsilon^{-k}\,e^{-\alpha(1-x)/\varepsilon} \qquad \text{for } k = 0, 1, \ldots, q. \tag{2.2}$$

– Discrete Maximum Principle:

LEMMA 2.2. *The discrete operator L^N satisfies a discrete maximum principle, i.e., if $\{v_i\}$ and $\{w_i\}$ are mesh functions that satisfy $v_0 \leq w_0$, $v_N \leq w_N$, and $L^N(v_i) \leq L^N(w_i)$ for $i = 1, \ldots, N-1$, then $v_i \leq w_i$ for all i.*

When the conditions of Lemma 2.2 are satisfied, we say that $\{w_i\}$ is a *barrier function* for $\{v_i\}$.

– Barrier Functions:

Set $\beta = \alpha/2$.

LEMMA 2.3. *Let $z_i := 1 + x_i$ for $i = 0, 1, \ldots, N$. Then $L^N(z_i) \geq \beta$, for $i = 1, \ldots, N-1$.*

LEMMA 2.4. *For $i = 0, \ldots, N$, define the mesh function*

$$S_i = \prod_{j=1}^{i} \left(1 + \frac{\beta h_j}{\varepsilon}\right)$$

(with the usual convention that if $i = 0$, then $S_0 = 1$). Then, for $i = 1, \ldots, N-1$, we have

$$L^N(S_i) \geq \frac{C}{\max\{\varepsilon, h_i\}} S_i \,,$$

for some positive constant C.

COROLLARY 2.1. *For the particular case when $L^N = L_1^N$, Lemma 2.4 still holds true if β is replaced by α in the definition of S_i.*

– Stability for the discrete operator L^N:

The following Lemma enables us to bound the pointwise error in terms of a discrete L_1 norm of the consistency error. In the terminology of [15], it says that L^N is $(\infty, 1)$-stable, just as the differential operator L is $(\infty, 1)$-stable because its Green's function is bounded pointwise.

LEMMA 2.5. *Write M_N for the $(N+1) \times (N+1)$ matrix of the difference scheme L^N, where the boundary conditions are handled by $(M_N)_{0,0} = 1$, $(M_N)_{0,i} = (M_N)_{N,i-1} = 0$ for $i = 1, \ldots, N$, and $(M_N)_{N,N} = 1$. Then for any $(N+1)$-dimensional row vector $v = (0, v_1, v_2, \ldots, v_{N-1}, 0)$, we have, for each i,*

$$|v_i| \leq C \sum_{j=1}^{N-1} h_j |(M_N v^T)_j|,$$

where T denotes transpose.

– Sharp estimate of the layer part:

LEMMA 2.6. *For each i and any constant $k > 0$, we have*

$$\exp\left(-\frac{k(1-x_i)}{\varepsilon}\right) \leq \prod_{j=i+1}^{N} \left(1 + \frac{kh_j}{\varepsilon}\right)^{-1} . \tag{2.3}$$

Now we formulate the main statement of this section.

THEOREM 2.1. *Let u be the solution of (1.1) and $\{u_i\}$ the solution of (1.3). Assume that H is sufficiently small (independently of ε). Then, for each i, we have*

$$\begin{aligned} |u(x_i) - u_i| \quad &\leq \quad CH(\varepsilon + H) + C\varepsilon \sum_{j=1}^{N-1} |\delta_{j+1/2} a_{j+1/2} - \delta_{j-1/2} a_{j-1/2}| \\ &\quad + C \prod_{j=i+1}^{N} \left(1 + \frac{\beta h_j}{\varepsilon}\right)^{-1} . \end{aligned} \tag{2.4}$$

We can sharpen this result for the special case of L_1^N.

COROLLARY 2.2. *Let u be the solution of (1.1) and $\{u_i\}$ the solution of (1.6) (i.e., the solution computed using L_1^N). Assume that H is sufficiently small (independently of ε). Then, for each i, we have*

$$|u(x_i) - u_i| \le CH(\varepsilon + H) + C\varepsilon \sum_{j=1}^{N-1} |h_{j+1} - h_j| + C \prod_{j=i+1}^{N} \left(1 + \frac{\beta h_j}{\varepsilon}\right)^{-1}.$$

Theorem 2.1 also implies the following simpler but weaker result for the general difference scheme L^N.

COROLLARY 2.3. *Let u be the solution of (1.1) and $\{u_i\}$ the solution of (1.3). Assume that H is sufficiently small (independently of ε). Then, for each i, we have*

$$|u(x_i) - u_i| \le C(\varepsilon + H^2) + C \prod_{j=i+1}^{N} \left(1 + \frac{\beta h_j}{\varepsilon}\right)^{-1}.$$

3. Estimate on a Shishkin Mesh

The accuracy of our computed solution will be improved if we use a mesh that (at least partly) resolves the boundary layer. Many adaptive and special meshes proposed in the literature set out to do this. (See [13] for a summary of previous work in this direction.) In particular, Shishkin [14] introduced piecewise uniform meshes of this type, which are simpler to handle than graded grids.

A Shishkin mesh for (1.1) is defined in the following way: let N be an even integer. Set

$$\tau = \min\left\{\frac{1}{2}, \frac{\tau_0}{\alpha}\varepsilon \ln N\right\},$$

where the constant τ_0 is independent of ε and N. Divide each of the intervals $[0, 1-\tau]$ and $[1-\tau, 1]$ into $N/2$ equidistant subintervals. In practice one usually has $\tau \ll 1$, so the mesh is coarse on $[0, 1-\tau]$ and fine on $[1-\tau, 1]$.

We shall assume that $\tau = (\tau_0/\alpha)\varepsilon \ln N$, as otherwise N is exponentially large relative to ε^{-1}, which is very unlikely in practice and implies that any reasonable numerical method will yield accurate results for (1.1). We denote the mesh width of each subinterval in $[1-\tau, 1]$ by h. Then it is easy to see that

$$N^{-1} \le H \le 2N^{-1} \quad \text{and} \quad h = \frac{2\tau_0}{\alpha}\varepsilon N^{-1} \ln N. \tag{3.1}$$

The simple structure of the Shishkin mesh allows us to express the result of Theorem 2.1 in a more accessible form for our special schemes L_1^N and L_2^N.

Our first theorem gives an estimate for the error in the solution computed by L_1^N, expressed in terms of the parameter τ_0, under a mild condition on the size of N (see Remark 3.1).

THEOREM 3.1. *Let u be the solution of (1.1). Let our mesh be the Shishkin mesh described above. Assume that H is sufficiently small (independently of ε) and that $\tau_0 N^{-1} \ln N \le 1$. Let $\{u_i\}$ be the solution computed by the scheme (1.6) that defines L_1^N. Then for each i we have*

$$|u(x_i) - u_i| \le C \max \left\{ N^{-\tau_0} \exp\left(\frac{16\tau_0^2}{e^2\sqrt{N}} \right), \tau_0 N^{-1} \ln N \right\}.$$

REMARK 3.1. *In practice one typically has $\tau_0 \in [1, 10]$, so our assumption that $\tau_0 N^{-1} \ln N \le 1$ is not restrictive.*

Now we move on to our alternative SDFEM, L_2^N. As we shall see in Theorem 3.2, its virtue is that on the Shishkin mesh it attains almost second-order accuracy when $\tau_0 \ge 2$. First we state a sharper version of Lemma 2.4 for L_2^N on the Shishkin mesh, under two mild conditions on N.

LEMMA 3.1. *For $i = 1, \ldots, N-1$, let S_i be the mesh function defined in Lemma 2.4 with β replaced by α. Assume that our mesh is the Shishkin mesh, that $\tau_0 N^{-1} \ln N < 2\alpha / \max_{[0,1]} a(\cdot)$ and that $2\varepsilon N \le \alpha$. Then, for $i = 1, \ldots, N-1$, we have*

$$L_2^N(S_i) \ge \frac{C}{\max\{\varepsilon, h_i\}} \, S_i,$$

for some positive constant C.

The conditions $\tau_0 N^{-1} \ln N < 2\alpha / \max_{[0,1]} a(\cdot)$ and $2\varepsilon N \le \alpha$ are reasonable in practice.

THEOREM 3.2. *Let u be the solution of (1.1). Let our mesh be the Shishkin mesh. Assume that H is sufficiently small (independently of ε) and that*

$$\tau_0 N^{-1} \ln N < 2\alpha / \max_{[0,1]} a(\cdot) \quad \text{and} \quad 2\varepsilon N \le \alpha.$$

Let $\{u_i\}$ be the solution computed by the scheme (1.4), (1.7) that defines L_2^N. Then for each i we have

$$|u(x_i) - u_i| \le C \max \left\{ N^{-\tau_0} \exp\left(\frac{16\tau_0^2}{e^2\sqrt{N}} \right), \tau_0^2 N^{-2} \ln^2 N \right\}.$$

REMARK 3.2. *Theorem 3.2 implies that for fixed $\tau_0 \ge 2$, we have the error bound*

$$\sup_{0<\varepsilon\le 1} \max_{0\le i\le N} |u(x_i) - u_i| \le M(\tau_0)\, N^{-2} \ln^2 N.$$

Thus the method is in practice almost second-order convergent, but the error constant M depends on the value of τ_0. We shall verify this by numerical experiments in the next section.

REMARK 3.3. *Under the hypotheses of Theorem 3.2, the scheme L_2^N is upwinded only on the coarse mesh; on $[1-\lambda, 1]$, where the layer is strongest, the fine Shishkin mesh is sufficient to stabilize the method.*

TABLE 4.1. SDFEM method, $\varepsilon = 10^{-4}$

τ_0	N=16	N=32	N=64	N=128	N=256	N=512	N=1024
0.2	3.9586e-03	7.2236e-04	1.2321e-03	2.3350e-03	4.1228e-03	7.1356e-03	1.2153e-02
0.4	1.2145e-02	1.0514e-02	7.4568e-03	4.7669e-03	2.8716e-03	2.0652e-03	3.0537e-03
0.6	2.6967e-02	1.9871e-02	1.2958e-02	7.9023e-03	4.6240e-03	2.6346e-03	1.4736e-03
0.8	3.9902e-02	2.8100e-02	1.7861e-02	1.0745e-02	6.2438e-03	3.5437e-03	1.9784e-03
1.0	5.1980e-02	3.5554e-02	2.2436e-02	1.3450e-02	7.8093e-03	4.4318e-03	2.4743e-03
1.2	6.1826e-02	4.2587e-02	2.6771e-02	1.6089e-02	9.3478e-03	5.3106e-03	2.9669e-03
1.4	7.2231e-02	4.8787e-02	3.1016e-02	1.8669e-02	1.0874e-02	6.1843e-03	3.4579e-03
1.6	8.2018e-02	5.5598e-02	3.5189e-02	2.1198e-02	1.2385e-02	7.0550e-03	3.9475e-03
1.8	9.0330e-02	6.1608e-02	3.9018e-02	2.3716e-02	1.3890e-02	7.9215e-03	4.4361e-03
2.0	9.7215e-02	6.6702e-02	4.3208e-02	2.6237e-02	1.5379e-02	8.7840e-03	4.9237e-03
2.2	1.0276e-01	7.2862e-02	4.6994e-02	2.8689e-02	1.6858e-02	9.6442e-03	5.4101e-03

TABLE 4.2. SDFEM method, $\varepsilon = 10^{-8}$

τ_0	N=16	N=32	N=64	N=128	N=256	N=512	N=1024
0.2	3.9266e-03	7.4012e-04	1.2360e-03	1.1446e-03	8.5073e-04	5.6533e-04	3.5158e-04
0.4	1.2177e-02	1.0545e-02	7.4869e-03	4.7934e-03	2.8937e-03	1.6832e-03	9.5508e-04
0.6	2.6997e-02	1.9897e-02	1.2979e-02	7.9176e-03	4.6350e-03	2.6423e-03	1.4791e-03
0.8	3.9932e-02	2.8122e-02	1.7876e-02	1.0754e-02	6.2496e-03	3.5472e-03	1.9805e-03
1.0	5.2006e-02	3.5572e-02	2.2447e-02	1.3456e-02	7.8129e-03	4.4338e-03	2.4754e-03
1.2	6.1853e-02	4.2603e-02	2.6781e-02	1.6094e-02	9.3507e-03	5.3122e-03	2.9678e-03
1.4	7.2253e-02	4.8805e-02	3.1025e-02	1.8674e-02	1.0877e-02	6.1859e-03	3.4587e-03
1.6	8.2043e-02	5.5613e-02	3.5199e-02	2.1203e-02	1.2388e-02	7.0566e-03	3.9484e-03
1.8	9.0357e-02	6.1626e-02	3.9029e-02	2.3722e-02	1.3893e-02	7.9233e-03	4.4371e-03
2.0	9.7245e-02	6.6722e-02	4.3219e-02	2.6244e-02	1.5382e-02	8.7860e-03	4.9247e-03
2.2	1.0280e-01	7.2879e-02	4.7006e-02	2.8695e-02	1.6862e-02	9.6463e-03	5.4112e-03

4. NUMERICAL EXPERIMENTS

All of our experiments have been performed on Shishkin meshes using the test problem

$$-\varepsilon u''(x) + (1 + x(1-x))\, u'(x) = f(x) \quad \text{on } (0,1), \quad u(0) = u(1) = 0, \tag{4.1}$$

where f is chosen such that

$$u(x) = \frac{1 - e^{-(1-x)/\varepsilon}}{1 - e^{-1/\varepsilon}} - \cos\frac{\pi}{2}x \tag{4.2}$$

is the exact solution. This solution exhibits typical boundary layer behaviour.

To construct our Shishkin mesh we have taken $\alpha = 1.0$ in all our examples. As we shall vary τ_0 below, there is no point in also varying α as only the quotient τ_0/α affects the placement of the mesh.

We shall study the rates of convergence for the SDFEM method for various choices of δ, viz., (1.5), (1.7) and (1.9). When δ is given by (1.5), we simply refer to the resulting method as the *SDFEM method*; when δ is defined by (1.7), we call the method the *SDFEM/Galerkin method*; and when δ comes from (1.9), we call the method the *exponentially fitted SDFEM*.

Tables 4.1 – 4.6 show the maximum nodal errors as τ_0 varies, for $\varepsilon = 10^{-4}$ and $\varepsilon = 10^{-8}$. The range of values for τ_0 is chosen so as to spread across the two convergence regimes appearing in Theorems 3.1 and 3.2.

In Figures 4.1 – 4.3 we show the results for $\varepsilon = 10^{-8}$ (the results for $\varepsilon = 10^{-4}$ are qualitatively similar). In Figures 4.1 and 4.2 we show the maximum nodal

TABLE 4.3. SDFEM/Galerkin method, $\varepsilon = 10^{-4}$

τ_0	N=16	N=32	N=64	N=128	N=256	N=512	N=1024
0.2	1.3495e-02	7.4173e-03	3.7919e-03	2.3180e-03	4.1032e-03	7.1140e-03	1.2130e-02
0.4	1.3295e-02	5.9575e-03	2.4994e-03	1.0215e-03	1.3474e-03	2.0404e-03	3.0310e-03
0.6	1.0767e-02	3.9505e-03	1.3699e-03	4.6801e-04	4.3947e-04	5.8434e-04	7.5714e-04
0.8	8.5223e-03	2.6555e-03	8.2288e-04	2.5515e-04	1.4009e-04	1.6631e-04	1.8879e-04
1.0	7.4269e-03	2.3737e-03	7.5361e-04	2.3725e-04	7.4005e-05	4.6283e-05	4.6724e-05
1.2	7.8940e-03	2.6544e-03	8.8510e-04	2.8740e-04	9.1378e-05	2.8541e-05	1.1213e-05
1.4	9.1636e-03	3.2429e-03	1.1148e-03	3.6907e-04	1.1874e-04	3.7296e-05	1.1486e-05
1.6	1.1242e-02	4.0688e-03	1.4114e-03	4.7068e-04	1.5240e-04	4.8007e-05	1.4799e-05
1.8	1.3533e-02	4.9962e-03	1.7532e-03	5.8899e-04	1.9130e-04	6.0325e-05	1.8602e-05
2.0	1.5928e-02	6.0782e-03	2.1547e-03	7.2329e-04	2.3489e-04	7.4140e-05	2.2868e-05
2.2	1.9489e-02	7.3961e-03	2.5759e-03	8.7261e-04	2.8315e-04	8.9433e-05	2.7587e-05

TABLE 4.4. SDFEM/Galerkin method, $\varepsilon = 10^{-8}$

τ_0	N=16	N=32	N=64	N=128	N=256	N=512	N=1024
0.2	1.3463e-02	7.3800e-03	3.7495e-03	1.8213e-03	8.6074e-04	3.9953e-04	1.8314e-04
0.4	1.3256e-02	5.9156e-03	2.4593e-03	9.8542e-04	3.8695e-04	1.5019e-04	5.7887e-05
0.6	1.0729e-02	3.9162e-03	1.3421e-03	4.4688e-04	1.4694e-04	4.8101e-05	1.5740e-05
0.8	8.4894e-03	2.6321e-03	8.0772e-04	2.4576e-04	7.4049e-05	2.2103e-05	6.5398e-06
1.0	7.4044e-03	2.3597e-03	7.4532e-04	2.3273e-04	7.1598e-05	2.1702e-05	6.4895e-06
1.2	7.8771e-03	2.6453e-03	8.8000e-04	2.8476e-04	9.0097e-05	2.7914e-05	8.4927e-06
1.4	9.1515e-03	3.2352e-03	1.1110e-03	3.6721e-04	1.1786e-04	3.6882e-05	1.1299e-05
1.6	1.1231e-02	4.0629e-03	1.4084e-03	4.6923e-04	1.5166e-04	4.7664e-05	1.4642e-05
1.8	1.3523e-02	4.9908e-03	1.7507e-03	5.8770e-04	1.9063e-04	6.0006e-05	1.8456e-05
2.0	1.5919e-02	6.0741e-03	2.1522e-03	7.2199e-04	2.3425e-04	7.3827e-05	2.2725e-05
2.2	1.9483e-02	7.3921e-03	2.5735e-03	8.7140e-04	2.8251e-04	8.9126e-05	2.7445e-05

TABLE 4.5. Exponentially fitted SDFEM, $\varepsilon = 10^{-4}$

τ_0	N=16	N=32	N=64	N=128	N=256	N=512	N=1024
0.2	1.3370e-02	7.3464e-03	3.7510e-03	1.8378e-03	8.8330e-04	4.2451e-04	2.0873e-04
0.4	1.2700e-02	5.7250e-03	2.4146e-03	9.8869e-04	4.0291e-04	1.6770e-04	7.3738e-05
0.6	9.5598e-03	3.5587e-03	1.2555e-03	4.3532e-04	1.5239e-04	5.5541e-05	2.1918e-05
0.8	6.7757e-03	2.1200e-03	6.3610e-04	1.8953e-04	5.7652e-05	1.8509e-05	6.5274e-06
1.0	4.8194e-03	1.3046e-03	3.4289e-04	9.0299e-05	2.4461e-05	7.0350e-06	2.2191e-06
1.2	3.5600e-03	8.6983e-04	2.1007e-04	5.1497e-05	1.3104e-05	3.5466e-06	1.0372e-06
1.4	2.7820e-03	6.4421e-04	1.5097e-04	3.6498e-05	9.2473e-06	2.4931e-06	7.1607e-07
1.6	2.3114e-03	5.2858e-04	1.2486e-04	3.0722e-05	7.9406e-06	2.1757e-06	6.2932e-07
1.8	2.0300e-03	4.6965e-04	1.1334e-04	2.8498e-05	7.4972e-06	2.0799e-06	6.0589e-07
2.0	1.8626e-03	4.3968e-04	1.0827e-04	2.7640e-05	7.3458e-06	2.0507e-06	5.9947e-07
2.2	1.7633e-03	4.2442e-04	1.0602e-04	2.7305e-05	7.2930e-06	2.0414e-06	5.9759e-07

TABLE 4.6. Exponentially fitted SDFEM, $\varepsilon = 10^{-8}$

τ_0	N=16	N=32	N=64	N=128	N=256	N=512	N=1024
0.2	1.3350e-02	7.3269e-03	3.7293e-03	1.8143e-03	8.5845e-04	3.9882e-04	1.8292e-04
0.4	1.2673e-02	5.6965e-03	2.3874e-03	9.6386e-04	3.8087e-04	1.4855e-04	5.7462e-05
0.6	9.5302e-03	3.5323e-03	1.2342e-03	4.1892e-04	1.4012e-04	4.6507e-05	1.5377e-05
0.8	6.7482e-03	2.0988e-03	6.2150e-04	1.7997e-04	5.1562e-05	1.4701e-05	4.1833e-06
1.0	4.7955e-03	1.2883e-03	3.3299e-04	8.4644e-05	2.1342e-05	5.3591e-06	1.3428e-06
1.2	3.5395e-03	8.5697e-04	2.0297e-04	4.7806e-05	1.1261e-05	2.6590e-06	6.3006e-07
1.4	2.7642e-03	6.3363e-04	1.4541e-04	3.3733e-05	7.9220e-06	1.8820e-06	4.5169e-07
1.6	2.2957e-03	5.1943e-04	1.2011e-04	2.8379e-05	6.8188e-06	1.6588e-06	4.0708e-07
1.8	2.0158e-03	4.6138e-04	1.0903e-04	2.6345e-05	6.4545e-06	1.5946e-06	3.9593e-07
2.0	1.8495e-03	4.3195e-04	1.0418e-04	2.5573e-05	6.3343e-06	1.5762e-06	3.9314e-07
2.2	1.7510e-03	4.1704e-04	1.0206e-04	2.5280e-05	6.2946e-06	1.5709e-06	3.9244e-07

FIGURE 4.1. SDFEM method, $\varepsilon = 10^{-8}$

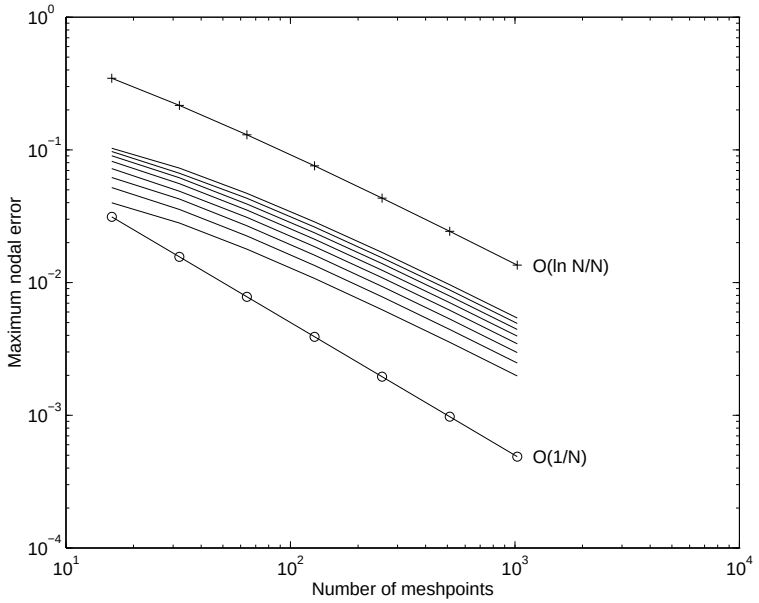

error in the solution (as a function of N) for the values $\tau_0 = 0.8, 1.0, \ldots, 2.2$, and in Figure 4.3 we take $\tau_0 = 0.2, 0.4, \ldots, 2.2$. We also draw two curves to illustrate certain fixed rates of convergence, so that the reader can make comparisons. In Figure 4.1 the lowest error curve is for $\tau_0 = 0.8$, and each increase of 0.2 in τ_0 moves us up to the next curve. In Figure 4.2, we see from the $N = 1024$ column in Table 4.4 that the same statement holds true if we look at the right-hand ends of the curves drawn, except that the curve $\tau_0 = 1.0$ lies below the curve for $\tau_0 = 0.8$. The order of curves in Figure 4.3, for the exponentially fitted SDFEM, is quite different; from the $N = 1024$ column in Table 4.6 it follows that, considering the right-hand end of each error curve, the highest curve is for $\tau_0 = 0.2$, and each increase of 0.2 in τ_0 moves us down to the next curve. We see from the Figure that as τ_0 increases, the method switches from first order to second order. But the exponentially fitted SDFEM is more computationally expensive than the other two methods, and we know from Theorem 3.2 that the simpler SDFEM/Galerkin method gives almost second-order convergence, so we do not consider a detailed theoretical analysis of the error behaviour of the exponentially fitted SDFEM. The (almost) first-order convergence and (almost) second-order convergence of the SDFEM and SDFEM/Galerkin methods can

FIGURE 4.2. SDFEM/Galerkin method, $\varepsilon = 10^{-8}$

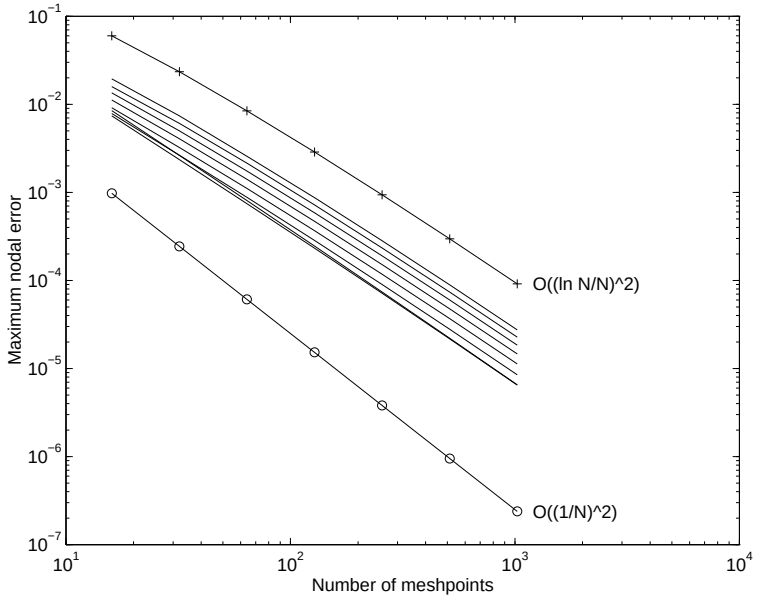

TABLE 4.7. SDFEM/Galerkin method, $\varepsilon = 0.005$

τ_0	N=16	N=32	N=64	N=128	N=256	N=512	N=1024
0.2	1.6790e-02	3.3015e-02	5.6024e-02	7.2884e-02	5.8146e-02	2.9610e-02	1.5159e-02
0.4	1.5121e-02	1.6028e-02	2.4123e-02	2.7422e-02	1.9009e-02	8.4340e-03	3.7543e-03
0.6	1.2519e-02	7.6398e-03	1.0339e-02	1.0307e-02	6.2180e-03	2.4068e-03	9.3366e-04
0.8	1.0012e-02	3.6593e-03	4.3649e-03	3.8528e-03	2.0313e-03	6.8946e-04	2.3534e-04
1.0	8.4908e-03	2.9707e-03	1.7720e-03	1.4175e-03	6.6023e-04	1.9994e-04	6.2364e-05
1.2	8.6369e-03	3.0518e-03	1.0215e-03	4.9842e-04	2.1120e-04	6.0349e-05	1.9468e-05
1.4	9.6807e-03	3.5334e-03	1.2123e-03	3.8987e-04	1.1739e-04	3.2124e-05	8.7822e-06
1.6	1.1692e-02	4.2803e-03	1.4869e-03	4.8764e-04	1.5050e-04	4.2795e-05	1.0795e-05
1.8	1.3926e-02	5.1821e-03	1.8137e-03	6.0353e-04	1.8902e-04	5.5040e-05	1.4565e-05
2.0	1.6269e-02	6.2147e-03	2.2114e-03	7.3625e-04	2.3217e-04	6.8767e-05	1.8798e-05
2.2	1.9707e-02	7.5225e-03	2.6294e-03	8.8379e-04	2.8001e-04	8.3961e-05	2.3489e-05

be seen clearly in Figures 4.1 and 4.2 respectively.

In all our experiments with the SDFEM and the SDFEM/Galerkin method, when we varied τ_0, we observed essentially the same behaviour: at first increasing τ_0 decreases the error, because we are in the $N^{-\tau_0}$ regime of Theorems 3.1 and 3.2, but eventually we move into the $\tau_0 N^{-1} \ln N$ or $\tau_0^2 N^{-2} \ln^2 N$ regime, where increasing τ_0 causes the error to increase.

Next, Figure 4.4 demonstrates what can happen when τ_0 has been chosen too small. The maximum nodal error of the SDFEM is studied for our test

FIGURE 4.3. Exponentially fitted SDFEM, $\varepsilon = 10^{-8}$

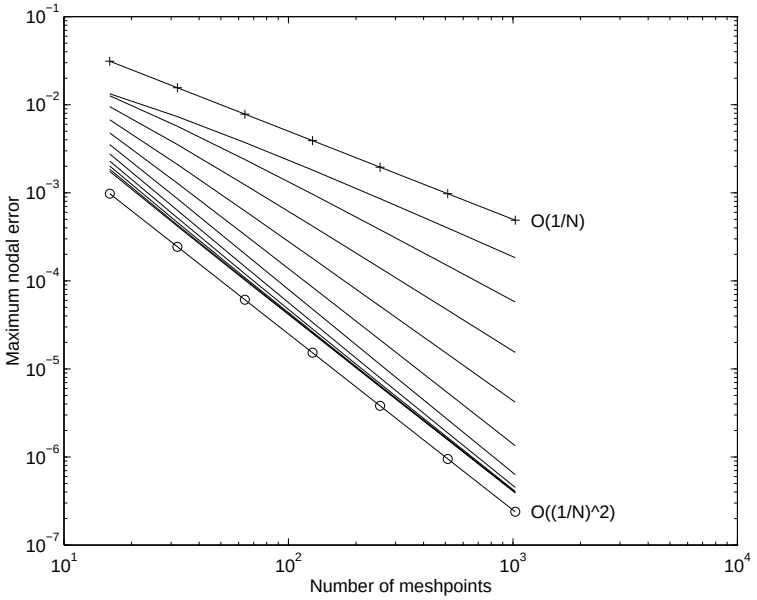

example (4.1) with $\varepsilon = 0.005$ and several values of τ_0. When τ_0 is too small, increasing the number of meshpoints first makes the error *increase*, then, after some threshold is passed, the error starts to decrease. This behaviour occurs because when τ_0 is very small, the coarse mesh intrudes on the boundary layer region and the method behaves like an upwind method on a uniform coarse mesh; in this setting, initially increasing N is known to increase the maximum nodal error (cf. [13, page 41, Fig. 2.1]). The data corresponding to this Figure are given in Table 4.7.

Finally, in Figure 4.5 we take $\varepsilon = 0.001$ and $N = 64$ and graph the maximum nodal error as a function of τ_0 for both the SDFEM and SDFEM/Galerkin methods.

The optimal value of τ_0 for each method is the value that yields the lowest point on the corresponding curve. We see in both cases that moving τ_0 below its optimal value leads rapidly to an unacceptably large error, but increasing τ_0 above this optimum causes a much slower increase in the error. This fits with the theoretical error bounds given in Theorems 3.1 and 3.2. Indeed, for larger values of τ_0 we can observe the convergence behaviours of $\tau_0 N^{-1} \ln N$ (i.e., linear in τ_0) and $\tau_0^2 N^{-2} \ln^2 N$ (i.e., quadratic in τ_0) that were predicted in these

FIGURE 4.4. SDFEM/Galerkin method, $\varepsilon = 0.005$

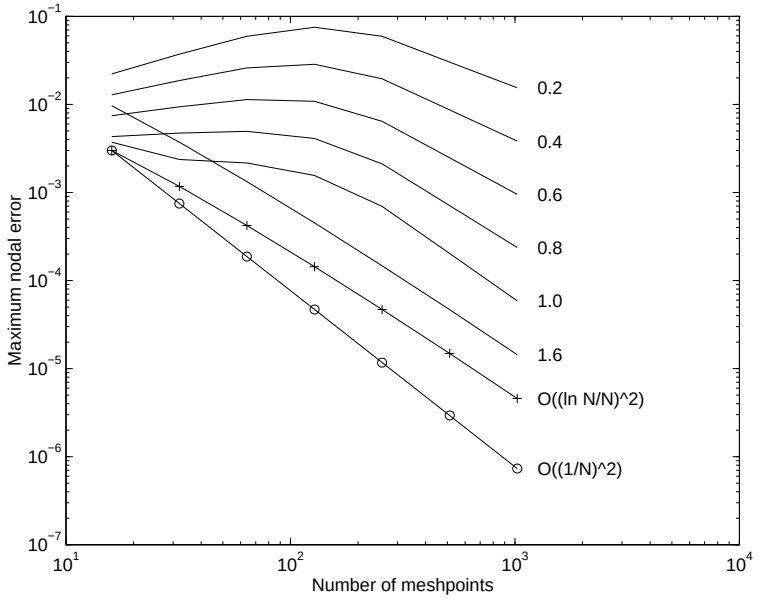

Theorems. Furthermore, because of the (almost) second-order convergence of the SDFEM/Galerkin method, its error is for reasonable τ_0 much smaller than the corresponding error of the SDFEM.

Our theory and experience lead us to conclude that the SDFEM/Galerkin method should always be used in preference to the SDFEM, and that as the optimal value of τ_0 is in practice unknown, it is wiser to choose τ_0 too large than too small.

REFERENCES

1. V.B. ANDREEV, I.A. SAVIN (1995). On uniform with respect to a small parameter convergence of a monotone scheme of A.A. Samarskij and its modification (in Russian). *Comput. Math. Math. Phys.* **35**, 739–752.
2. A.F. HEGARTY, J.J.H. MILLER, E. O' RIORDAN and G.I. SHISHKIN (1994). On numerical experiments with central difference operators on special piecewise uniform meshes for problems with boundary layers. W. HACKBUSCH and G. WITTUM, editors, *Adaptive Methods – Algorithms, Theory and Applications. Proceedings 9th GAMM Seminar, Kiel, January 22-24, 1993*, volume **46**, of *Notes on Numerical Fluid Dynamics*, Braun-

FIGURE 4.5. SDFEM and SDFEM/GALERKIN for $N = 64$ and $\varepsilon = 0.001$

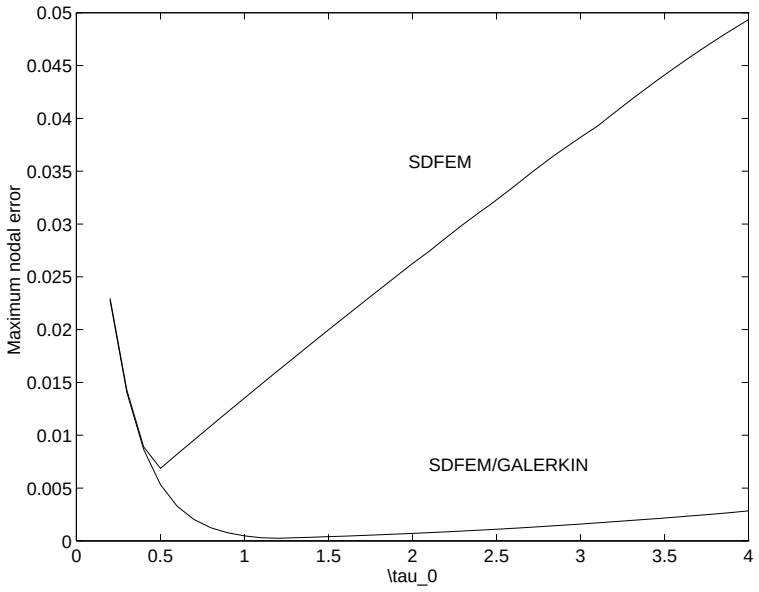

schweig, Vieweg.

3. T.J.R. HUGHES (1995). Multiscale phenomena: Green's functions, the Dirichlet-to-Neumann formulation, subgrid scale models, bubbles and the origins of stabilized methods. *Comp. Methods Appl. Mech Engrg.*, **127**, 387–401.
4. T.J.R. HUGHES, A.N. BROOKS (1979). A multidimensional upwind scheme with no crosswind diffusion. T.J.R. HUGHES, editor, *Finite Element Methods for Convection Dominated Flows*, volume **34** of *AMD*. ASME, New York.
5. V. JOHN, J. M. MAUBACH and L. TOBISKA. Nonconforming streamline-diffusion finite element methods for convection-diffusion problems. *Numer. Math.*, to appear.
6. C. JOHNSONA, J. SARANEN (1986). Streamline diffusion methods for the incompressible Euler and Navier–Stokes equations. *Math. Comp.* **47**, 1–18.
7. C. JOHNSON, A.H. SCHATZ and L.B. WAHLBIN (1987). Crosswind smear and pointwise errors in the streamline diffusion finite element methods. *Math. Comp.* **49**, 25–38.
8. G. LUBE, L. TOBISKA (1990). A nonconforming finite element method of

streamline-diffusion type for the incompressible Navier-Stokes equations. *J. Comp. Math.*, **8**, 147–158.
9. J.J. Miller, E. O'Riordan and G.I. Shishkin (1996). *Fitted Numerical Methods for Singular Perturbation Problems.* World Scientific, Singapore.
10. U. Nävert (1982). *A finite element method for convection-diffusion problems.* PhD thesis, Chalmers University of Technology, Göteborg.
11. K. Niijima (1990). Pointwise error estimates for a streamline diffusion finite element scheme. *Numer. Math.* **56**, 707–719.
12. R.E. O'Malley (1991). *Singular Perturbation Methods for Ordinary Differential Equations.* Springer-Verlag, New York.
13. H.-G. Roos, M. Stynes and L. Tobiska (1996). *Numerical Methods for Singularly Perturbed Differential Equations.* Springer-Verlag, Berlin Heidelberg New York.
14. G.I. Shishkin (1988). Difference scheme for a singularly perturbed parabolic equation with discontinuous boundary conditions (in Russian). *Comput. Math. and Math. Phys.* **28**, 1679–1692.
15. M. Stynes, E. O'Riordan (1989). Analysis of singularly perturbed two-point boundary value problems with turning points. *Proc. Discretization Methods of Singular Problems and Flow Problems*, (L. Tobiska, ed.), 81–88.
16. M. Stynes, H.-G. Roos (1997). The midpoint upwind scheme. *Appl. Numer. Math.* **23**, 361–374.
17. M. Stynes, L. Tobiska (1997). *Analysis of streamline-diffusion-type methods on arbitrary and shishkin meshes.* Department of Mathematics Preprint 1997-3, University College Cork.
18. L. Tobiska, R. Verfürth (1996). Analysis of a streamline diffusion finite element method for the Stokes and Navier–Stokes equations. *SIAM J. Numer. Anal.* **33**, 107–127.
19. G. Zhou (1997). How accurate is the streamline diffusion finite element method? *Math. Comp.* **66**, 31–44.